

Inversions shape the divergence of *Drosophila pseudoobscura* and *D. persimilis* on multiple timescales

1 **Abstract**

2 By shaping meiotic recombination, chromosomal inversions can influence genetic exchange between
3 hybridizing species. Despite the recognized importance of inversions in evolutionary processes such
4 as divergence and speciation, teasing apart the effects of inversions over time remains challenging.
5 For example, are their effects on sequence divergence primarily generated through creating blocks of
6 linkage-disequilibrium pre-speciation or through preventing gene flux after speciation? We provide a
7 comprehensive look into the influence of inversions on gene flow throughout the evolutionary
8 history of a classic system: *Drosophila pseudoobscura* and *D. persimilis*. We use extensive whole-genome
9 sequence data to report patterns of introgression and divergence with respect to chromosomal
10 arrangements. Overall, we find evidence that inversions have contributed to divergence patterns
11 between *Drosophila pseudoobscura* and *D. persimilis* over three distinct timescales: 1) segregation of
12 ancestral polymorphism early in the speciation process, 2) gene flow after the split of *D. pseudoobscura*
13 and *D. persimilis*, but prior to the split of *D. pseudoobscura* subspecies, and 3) recent gene flow between
14 sympatric *D. pseudoobscura* and *D. persimilis*, after the split of *D. pseudoobscura* subspecies. We discuss
15 these results in terms of our understanding of evolution in this classic system and provide cautions
16 for interpreting divergence measures in other systems.

17

18 **Keywords:** inversions, introgression, divergence, recombination, speciation

19

20 ***Introduction***

21 Divergence and speciation sometimes occur in the presence of gene exchange between taxa.
22 Estimates suggest that over 10% of animal species hybridize and exchange genes with related species
23 (Mallet, 2005). Analyses in the genomic era have provided further evidence of the widespread
24 prevalence of hybridization and revealed many previously unanticipated instances of hybridization
25 (Payseur & Rieseberg, 2016; Taylor & Larson, 2019). Understanding genetic exchange between
26 species gives us insights into the genetic processes underlying later stages of the speciation
27 continuum. Many approaches can examine evidence for introgression, including comparing
28 sympatric vs. allopatric populations to test for differences in nucleotide divergence. Other available
29 methods for characterizing gene flow include model-based frameworks and examinations of
30 differences in divergence reflected in coalescence times. Differences in coalescence times are often
31 observed between species in regions where recombination is limited in hybrids, such as fixed
32 chromosomal inversion differences (Guerrero, Rousset, & Kirkpatrick, 2012). When species
33 differing by inversions hybridize, the collinear genomic regions can freely recombine, while inverted
34 regions experience severely limited genetic exchange in hybrids and often accumulate greater
35 sequence differentiation over generations. This process can lead to locally adapted traits and
36 reproductive isolating barriers mapping disproportionately to inverted regions (reviewed in Ayala &
37 Coluzzi 2005; Butlin 2005; Jackson 2011).

38 Many studies examine the timing and frequency of gene exchange between hybridizing
39 species, with emphasis on the implications of patterns of divergence in allopatric vs sympatric pairs
40 and in regions of reduced recombination in hybrids. However, different approaches sometimes
41 yield distinct interpretations regarding the presence or extent of introgression. Model-based
42 approaches yield important insights but are also limited in the scenarios that they consider and the

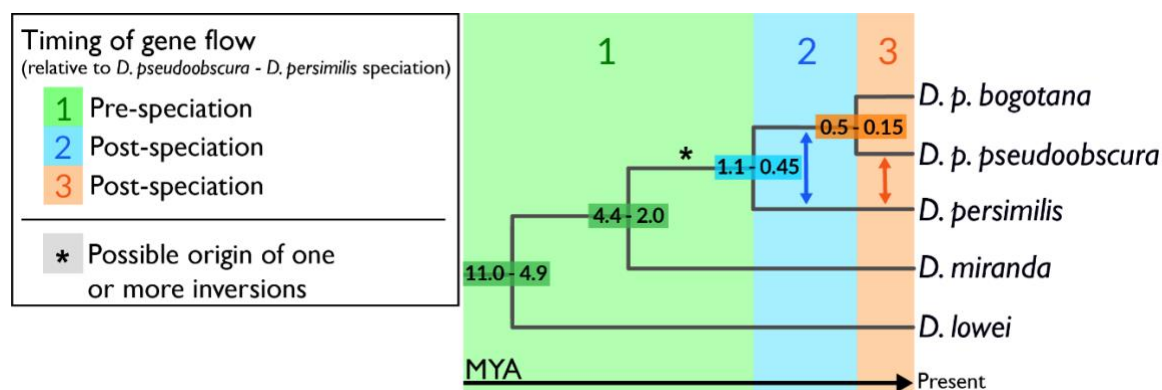
43 assumptions they make about population histories and evolutionary rates (reviewed in Payseur &
44 Rieseberg 2016). Further, shared patterns of variation are often interpreted as evidence of ongoing
45 gene flow, but segregating ancestral polymorphism could also be the primary, or even the sole,
46 driver of these patterns (Fuller, Leonard, Young, Schaeffer, & Phadnis, 2018). In the ancestral
47 population of two species, segregating chromosomal inversions may shield inverted regions of the
48 genome from recombination, thus facilitating the divergence of sympatric ecotypes or populations.
49 Heightened within-species differentiation in inverted regions has been observed in many systems,
50 including *Rhagoletis pomonella* (Michel et al., 2010), *Anopheles gambiae* (Manoukis et al., 2008), and
51 *Mimulus guttatus* (Lowry & Willis, 2010). Such heightened differentiation between karyotypes may
52 persist along the speciation continuum, making it difficult to disentangle the effects of inversions
53 reducing recombination in the ancestral population vs reducing introgression upon secondary
54 contact. Fuller *et al.* (2018) recently discussed the possibility that ancestrally segregating inversions
55 that sort between species may provide a "head-start" in molecular divergence, possibly predisposing
56 them to harbor a disproportionate fraction of alleles associated with species differences. Unlike
57 models assuming homogenization of collinear regions via post-speciation gene flow, this model
58 predicts that young species that diverged in allopatry may also exhibit higher divergence in inverted
59 regions than collinear regions. These models are not mutually exclusive: dynamics of the ancestral
60 population as well as post-speciation gene flow can shape patterns of variation between species.

61 Disentangling the effects of ancestral polymorphism from the effects of post-speciation gene
62 flow is a fundamental puzzle in understanding speciation. To achieve a cohesive picture of how
63 hybridization influences divergence and speciation, we need to consider the approaches outlined
64 above in a model system with extensive whole-genome sequence data to assess models and reconcile
65 interpretations of possible signals of introgression. The sister species pair *Drosophila pseudoobscura* and
66 *D. persimilis* present an ideal opportunity to dissect an evolutionary history of divergence nuanced by

67 multiple inversions, lineage sorting, and gene flow. Despite the rich history of work on
68 understanding speciation and divergence in *D. pseudoobscura* and *D. persimilis*, there are unresolved
69 questions about the rates and timing of introgression between these species. A few F₁ hybrids of
70 these species have been collected in the wild (Powell 1983) and many previous studies have
71 documented molecular evidence of introgression, detectable in both nuclear and mitochondrial loci
72 (e.g., Machado *et al.* 2002; Machado & Hey 2003; Hey & Nielsen 2004; Fuller *et al.* 2018). Inverted
73 regions between these species exhibit greater sequence differences than collinear regions, and this
74 pattern was previously inferred to result from introgression post-speciation. McGaugh and Noor
75 (2012) used multiple genome sequences of both species and an outgroup, and reinforced previous
76 studies (e.g., Noor *et al.* 2007) showing that the three chromosomal inversions differ in divergence
77 time. They inferred a "mixed mode geographic model" (Feder, Gejji, Powell, & Nosil, 2011) with
78 sporadic periods of introgression during and after the times that the inversions spread. However, in
79 addition to confirming evidence for gene flow between *D. pseudoobscura* and *D. persimilis* after
80 speciation, Fuller *et al.* (2018) recently argued the inversions arose within a single ancestor species,
81 differentially sorted in the descendant species, and this sorting of ancestral polymorphisms may
82 explain observed patterns of nucleotide variation. To fully understand the role of hybridization in
83 the speciation process, the contrasting models must be reconciled.

84 We acquired extensive whole-genome sequence data to re-explore patterns of introgression
85 and divergence in the *Drosophila pseudoobscura* / *D. persimilis* system. We leverage the allopatric *D.*
86 *pseudoobscura* subspecies, *D. pseudoobscura bogotana* (*D. p. bogotana*) and two outgroup species (*D. miranda*
87 and *D. lowei*) to distinguish recent from ancient effects of inversions on gene flow. Note that we use
88 *D. pseudoobscura* to refer to both *D. pseudoobscura* subspecies (*D. pseudoobscura pseudoobscura* and *D.*
89 *pseudoobscura bogotana*), and we specify *D. p. pseudoobscura* or *D. p. bogotana* when we are specifically
90 referring to only one of the two. Much of the previous support for post-speciation gene flow

between these species has focused on comparisons of *D. persimilis* and *D. p. pseudoobscura* (Fuller et al., 2018; Hey & Nielsen, 2004; Kulathinal, Steviston, & Noor, 2009; Machado et al., 2002; R. L. Wang, Wakeley, & Hey, 1997). In addition to analyzing *D. persimilis* and *D. p. pseudoobscura* genomes, we sequenced multiple strains of *D. p. bogotana* to provide a comparative dataset that allows us to clarify the role of inversions over the evolutionary history of these species by considering three distinct time scales: 1) pre-speciation segregation of ancestral polymorphism, 2) post-speciation ancient gene flow, and 3) recent introgression (Figure 1). In this context, we use pre- and post-speciation to refer to estimated divergence times of *D. persimilis* and *D. pseudoobscura*, though we note that speciation is a continuum and the present study does not address the emergence of reproductive isolation or the degree of species barriers. Patterns of divergence between *D. persimilis* and allopatric *D. p. bogotana* can be explained by the effects of segregating ancestral polymorphism and by gene flow prior to the split of *D. p. bogotana* (Figure 1, green and blue regions). In comparing the sympatric species, *D. persimilis* and *D. p. pseudoobscura*, the same forces factor into patterns of divergence, with the added effects of recent or ongoing gene flow (Figure 1, orange arrows). We leverage these two comparisons to weigh the relative contributions of recent genetic exchange.



106

Figure 1 | Gene flow in the context of the evolutionary history of *D. pseudoobscura* and *D. persimilis*. We consider how inversions differing between *D. pseudoobscura* and *D. persimilis* might shape patterns of divergence by affecting recombination at 3 timescales: 1) prior to the estimated

110 split of *D. pseudoobscura* and *D. persimilis*, by shaping recombination in populations with segregating
111 inversion polymorphisms, 2) after the split of *D. pseudoobscura* and *D. persimilis*, but prior to the split
112 of subspecies *D. p. pseudoobscura* and *D. p. bogotana*, and 3) during recent introgression between *D. p.*
113 *pseudoobscura* and *D. persimilis*. Here, we show the evolutionary context and approximate divergence
114 times of the taxa considered in the present study, with arrows indicating gene flow between *D.*
115 *pseudoobscura* and *D. persimilis*. Node ages are summarized from the literature for the divergence of
116 subspecies *D. p. pseudoobscura* and *D. p. bogotana* (S W Schaeffer & Miller, 1991; R. L. Wang & Hey,
117 1996), the divergence of *D. pseudoobscura* and *D. persimilis* (Fuller et al., 2018; Hey & Nielsen, 2004; R.
118 L. Wang & Hey, 1996), the divergence of *D. miranda* from the clade that contains *D. pseudoobscura* and
119 *D. persimilis* (Beckenbach, Wei, & Liu, 1993; R. L. Wang & Hey, 1996), and the divergence of *D. lowei*
120 from the rest of the group (Beckenbach et al., 1993).

121 We first examine patterns of divergence in inverted regions compared to collinear regions,
122 and we discuss evidence for segregation of inversion polymorphisms early in the speciation
123 continuum. We next examine evidence of post-speciation gene flow to test whether some of this
124 genetic exchange predates the split of *D. p. bogotana*, and we discuss signals of possible introgression
125 in the past 150,000 years since the split of the allopatric *D. p. bogotana*, from North American *D.*
126 *pseudoobscura* (*D. p. pseudoobscura*) (S W Schaeffer & Miller, 1991). Kulathinal *et al.* (2009) previously
127 argued that recent post-speciation gene flow contributes to the difference in coalescence time
128 between inverted and collinear regions, observable in the higher genetic similarity in collinear
129 regions between *D. persimilis* and sympatric *D. p. pseudoobscura* compared to similarity between *D.*
130 *persimilis* and allopatric *D. p. bogotana*. That study also tested for an excess of shared, derived bases
131 between *D. persimilis* and *D. p. pseudoobscura* compared to *D. persimilis* and allopatric *D. p. bogotana*.
132 Their application of this D-statistic precursor suggested a borderline statistically significant signature
133 of gene flow, but this test was limited by low sequencing coverage. Using recent statistical
134 approaches applied to high-coverage resequencing, we compare the sympatric (*D. p. pseudoobscura*)
135 and allopatric (*D. p. bogotana*) subspecies in their similarity to *D. persimilis*. Our estimation of
136 Patterson's D-statistic and f_d (Martin, Davey, & Jiggins, 2015) indicates very recent gene exchange in
137 collinear regions. Perhaps surprisingly, divergence measures to *D. persimilis* are also higher for

138 allopatric than sympatric *D. pseudoobscura* subspecies in *both* inverted and collinear regions. We
139 discuss several possible explanations for this pattern, including 1) extensive recent gene exchange
140 throughout much of the genome, even in inverted regions, 2) the role of segregating inversions in
141 ancestral populations, and 3) differences in evolutionary rates across taxa. We discuss these results in
142 the context of the extensive past work towards understanding divergence and speciation in this
143 classic system, and we provide cautions for interpreting divergence measures in other systems.

144 **Methods**

145 **Genomic datasets**

146 Whole-genome short-read sequence data were analyzed from 19 *D. p. pseudoobscura* and 8 *D.*
147 *persimilis* strains, along with 4 *D. p. bogotana* strains as an allopatric point of comparison. Both males
148 and females were sequenced, all from inbred strains listed in Supplementary Table 1 with SRA
149 accessions (Korunes, Myers, Hardy, & Noor, 2020; McGaugh et al., 2012; Samuk, Manzano-
150 Winkler, Ritz, & Noor, 2020). We used *D. lownei* as an outgroup. *D. lownei* likely diverged from the rest
151 of the *D. pseudoobscura* subgroup 5-11 MYA (Beckenbach et al., 1993), and hybrids between these
152 two species are sterile (Heed, Crumpacker, & Ehrman, 1969). Scripts used for genome alignment,
153 SNP calling, and analyses are available on GitHub
154 (https://github.com/kkorunes/Dpseudoobscura_Introgression). To avoid biasing identification of
155 variants towards *D. pseudoobscura*, the *D. miranda* reference genome assembly (DroMir2.2; GenBank
156 assembly accession GCA_000269505.2) was chosen as the reference for all ~~subsequent~~ alignments.
157 *D. miranda* diverged from *D. pseudoobscura* only within the past 2-4 million years (Beckenbach et al.,
158 1993; R. L. Wang & Hey, 1996), facilitating alignment of *D. pseudoobscura* and *D. persimilis* genomes to
159 the *D. miranda* genome assembly. Further, the arrangement of the assembled *D. miranda*
160 chromosomes matches the published contig order and arrangement of *D. pseudoobscura* (Stephen W.

161 Schaeffer *et al.*, 2008), but with the advantage of being assembled into 6 continuous chromosome
162 arms: chromosomes XL, XR, 2, 3, 4, and 5. Here, we analyze the majority (83%) of the assembled
163 genome. We exclude only regions where we cannot reasonably examine introgression and
164 divergence: chromosome 3, which presents confounding factors from its inversion polymorphisms
165 within species, including over 30 inversion polymorphisms known to segregate within *D.*
166 *pseudoobscura* and *D. persimilis* (Dobzhansky & Epling, 1944; Jeffrey R Powell, 1992), and the very
167 small (<2 Mb) portion of the genome found on the largely nonrecombining “dot” chromosome
168 (chromosome 5).

169 **Alignments and variant calling**

170 To confirm the arrangement of *D. pseudoobscura* contigs with respect to the *D. miranda*
171 reference, each *D. pseudoobscura* chromosome was split into lengths of 1 Mb, and these segments
172 were aligned to the *D. miranda* reference using BWA-0.7.5a (Li & Durbin, 2009). We then extracted
173 the 2 kb regions surrounding published inversion breakpoints to obtain the breakpoint locations in
174 the coordinates of the *D. miranda* reference (see Supplementary Table 2). After confirming that the
175 arrangement of the assembled *D. miranda* chromosomes matched the arrangement of the *D.*
176 *pseudoobscura* contig order and arrangement described by Schaeffer *et al.* (2008), all sequencing data
177 were aligned to the reference genome of *D. miranda* using BWA-0.7.5a (Li & Durbin, 2009), and
178 Picard command line tools were used to mark adapters and duplicates
179 (<http://broadinstitute.github.io/picard>). Unphased SNPs were called using GATK v4 and filtered
180 based on GATK’s hard filtering recommendations (McKenna *et al.*, 2010; Van der Auwera *et al.*, 2013),
181 excluding sites with QualByDepth (QD) < 2.0, FisherStrand (FS) > 60, StrandOddsRatio (SOR) >
182 3.0, MQ < 40, MQRankSum < -12.5, ReadPosRankSum < -8.

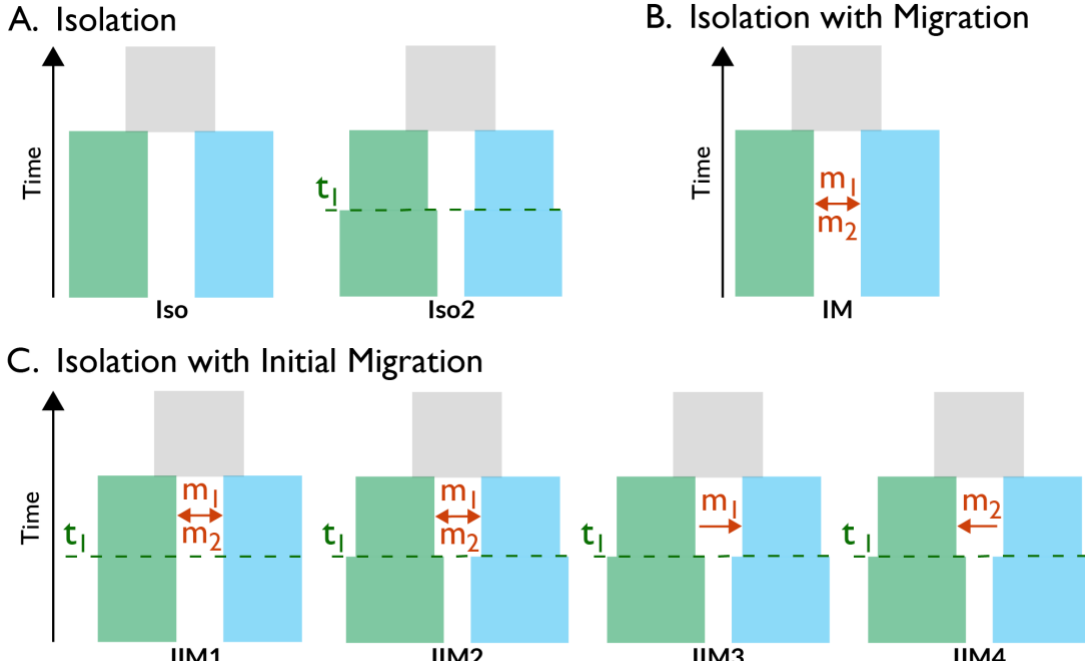
183 **Patterns of divergence**

184 The resulting VCF files were then processed using PLINK (Purcell et al., 2007). VCFs were
185 converted to PLINK's bed/bim format, keeping only sites that passed the filters described above.
186 SNPs were pruned for linkage disequilibrium using the --indep-pairwise function of PLINK ("--
187 indep-pairwise 50 50 0.5") before performing principal components analysis (PCA) using PLINK's -
188 -pca function to confirm the grouping of individuals within their respective species (Figure 1;
189 Supplementary Figure 1). Admixtools was used to estimate Patterson's D-statistic (Patterson et al.,
190 2012) using *D. lowei* as an outgroup to polarize ancestral vs derived alleles. For input into
191 Admixtools, we used the *convert* program of Admixtools to convert each PLINK ped file to
192 Eigenstrat format which includes a *genotype* file, a *snp* file, and an *indiv* file. Per recommendations in
193 the Admixtools documentation, we defined the physical positions of each SNP in the *snp* file to be
194 10 kb apart from each adjacent SNP to allow Admixtools to interpret every 100 SNPs as 1 Mb or
195 1cM, since this software uses centiMorgans as the unit for block size during jackknifing and assumes
196 that 1 Mb = 1 cM. We set the block size parameter to 0.01 cM, which in this case is interpreted as
197 blocks of 100 SNPs. Next, *qpDstat* was used to obtain D-statistics for each chromosome. These
198 four-population tests were of the form (((A,B), C), D), where A = *D. p. bogotana*, B = *D. p.*
199 *pseudoobscura*, C = *D. persimilis*, and D = *D. lowei*. To study signatures of introgression along the
200 genome, we applied f_d (Martin et al., 2015) in genomic intervals that presented an excess of ABBA
201 over BABA sites. Using non-overlapping windows of 100 SNPs, we calculated f_d using the
202 Dinvestigate program from Dsuite (Malinsky, Matschiner, & Svardal, 2020). Absolute divergence,
203 D_{xy} , was calculated using custom scripts over fixed window sizes of 50 kb. D_{xy} was calculated from
204 variant and invariant sites after subjecting SNPs to the filters described above and filtering invariant

205 sites based on depth (depth ≥ 10). Per-site depths for all sites were acquired from BAM files using
206 Samtools (“samtools depths -a <in>”) (Li et al., 2009).

207 **Models of gene flow**

208 To test for evidence of gene flow after the split of *D. pseudoobscura* and *D. persimilis*, but
209 before the split of *D. p. bogotana*, we used the maximum-likelihood methods derived by Costa &
210 Wilkinson-Herbots (2017) to compare scenarios of divergence between *D. persimilis* and *D. p.*
211 *bogotana* (Figure 2). We first considered models of divergence in isolation without gene flow
212 following the split of an ancestral population (Figure 2A) either with constant population size (Iso)
213 or allowing changes in population size (Iso2). We then considered a model of divergence in
214 isolation-with-migration (IM) with constant (but potentially asymmetric) gene flow since the split of
215 an ancestral population until the present (Figure 2B), and finally we considered four scenarios of
216 divergence in isolation-with-initial-migration (IIM) with gene flow until some timepoint in the past
217 and divergence in isolation since that timepoint (Figure 2C).



218

219 **Figure 2 | Models of Divergence.** We considered the following coalescent models described by
 220 Costa & Wilkinson-Herbots (2017) to consider scenarios of divergence of *D. persimilis* and *D. p.*
 221 *bogotana* (represented by the left and right lineages, respectively) since the split of the ancestral
 222 population (gray box): (A) divergence in isolation without gene flow, with either constant population
 223 sizes (Iso) or allowing changes in population sizes (Iso2); (B) divergence in isolation-with-migration
 224 (IM) with constant (but potentially asymmetric) gene flow; and (C) divergence in isolation-with-
 225 initial-migration (IIM) with gene flow until some timepoint (t_1) in the past. Under the IIM model, we
 226 tested the four scenarios shown from left to right: the first scenario (IIM2) assumes constant
 227 population sizes, the second (IIM2) allows for changes in population sizes, and the third (IIM3) and
 228 fourth (IIM4) allow for changes in population size but assume unidirectional gene flow.

229 We computed the likelihood of our *D. persimilis* and *D. p. bogotana* sequence data under each
 230 of the seven scenarios described above and in Figure 2 (Iso, Iso2, IM, IIM1, IIM2, IIM3, and IIM4).
 231 To reduce potential effects of selection, we used intergenic loci spaced at least 2 kb apart, similar to
 232 the strategy of Wang & Hey (2010), which similarly utilized diploid genome sequences from inbred
 233 lines of another *Drosophila* species pair and served as the empirical dataset used to illustrate the
 234 methods in Costa & Wilkinson-Herbots (2017). Linkage-disequilibrium decays within tens to
 235 hundreds of bases in *Drosophila* (Langley, Lazzaro, Phillips, Heikkinen, & Braverman, 2000), so we
 236 expect that avoiding genic regions will minimize the effects of linked selection. To identify intergenic

237 regions in the *D. miranda* genome, we used the set of all *D. pseudoobscura* gene annotations published
238 by Flybase (<http://flybase.org>, Full Annotation Release 3.04), and we used BLAST to identify
239 genomic regions with significant similarity to the *D. pseudoobscura* gene annotations, using cutoffs of
240 $\text{evalue} = 10^{-6}$ and percent identity = 80 (Altschul, Gish, Miller, Myers, & Lipman, 1990). From the
241 remaining regions, we then randomly sampled 500 bp segments separated by at least 2 kb to create a
242 set of \sim 15,000 intergenic loci. To ensure that our results were robust against the effects of linkage
243 within inverted regions, we sampled regions expected to be freely-recombing throughout the
244 timescales examined: i.e., we excluded any loci from the inverted regions, leaving \sim 11,000 intergenic,
245 collinear loci. We then randomly divided these loci into three nonoverlapping subsets to satisfy the
246 models' requirement of independent estimates of pairwise differences and mutation rates in loci (1)
247 within *D. persimilis*, (2) within *D. p. bogotana*, and (3) between *D. persimilis* and *D. p. bogotana*. Costa &
248 Wilkinson-Herbots (2017) recommends using per-locus relative mutation rates, which we calculated
249 using the average distance to the outgroup *D. lowei*, following the equation from Yang (2002), which
250 gives the relative mutation rate at a locus as the outgroup distance at that locus divided by the
251 average outgroup distance along all loci. To select the model that best fits the data, we then tested
252 the relative support among nested divergence models using likelihood-ratio tests following the
253 sequence of pairwise comparisons shown in Table 1, where the degrees of freedom in each test is
254 the difference in the number of parameters between alternative models (Costa & Wilkinson-
255 Herbots, 2017).

256 **Tests for differences in evolutionary rate**

257 Finally, to test for differences in evolutionary rate that might influence observed patterns of
258 divergence and gene flow, differences in substitution rates among the lineages were assessed with
259 Tajima's relative rate test, using *D. lowei* as the outgroup (Tajima 1993; scripts available on GitHub

repository linked above). Tajima's relative rate test was applied to the combined set of SNPs from chromosomes 2, 4, XL, and XR—excluding sites where the outgroup *D. lowei* was heterozygous or missing data. We next inferred relative clock rates within the tree using coalescent phylogenetic inference in StarBEAST2, a method specifically designed for multilocus genomic datasets (Ogilvie, Bouckaert, & Drummond, 2017). To choose a dataset similar to the empirical dataset shown to perform well in Ogilvie et al. (2017), we took a subset of 20 autosomal loci from the 500 bp collinear, intergenic loci used to test the coalescent models above. To enable estimation of per-species clock rates, we used an uncorrelated log-normal clock model (UCLN). The site models were set to the HKY substitution model, and the phylogenetic relationship was reconstructed under the default Yule process. StarBEAST2 was run using a chain length of 100 million, sampled every 1,000 generations, yielding an effective sample size >200 for the posterior of each parameter. The TreeAnnotator program provided with BEAST was used to calculate the posterior expectation and 95% credibility intervals of per-species clock rates, and a summary tree of the posterior distribution was visualized in FigTree v1.4.4 (Rambaut, 2018). For alignments used and all StarBEAST2 parameters, the xml is provided in the GitHub repository linked above.

275 **Results**

276 **Patterns of divergence in inverted vs collinear regions**

277 The suppression of crossing over within inversions leads to distinct signatures of nucleotide divergence within and near inversions. One of the advantages of this system for studying the evolutionary effects of chromosomal inversions is the existence of *D. p. bogotana*: a clear allopatric point of comparison for the North American *D. persimilis* and *D. p. pseudoobscura*. By including 4 *D. p. bogotana* genomes, we were able to compare patterns of divergence for both *D. persimilis* vs *D. p. pseudoobscura* and *D. persimilis* vs. *D. p. bogotana*. Figure 3 presents windowed divergence between *D. p. pseudoobscura* and *D. persimilis*.

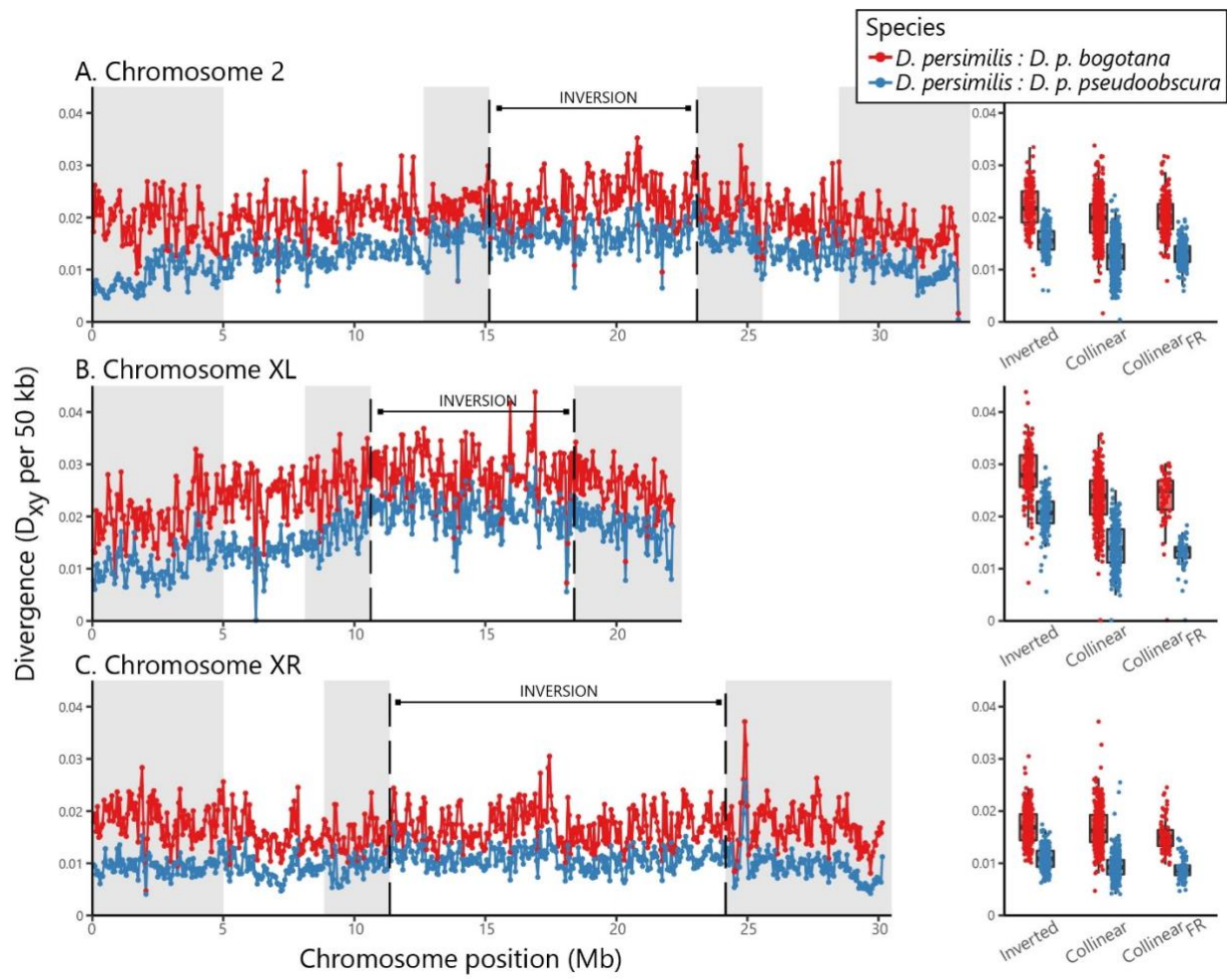
283 *persimilis* and *D. p. bogotana* and divergence between *D. persimilis* vs *D. p. pseudoobscura* for the three
284 chromosome arms that contain fixed (chromosome 2, XL) or nearly-fixed (chromosome XR)
285 inversion differences between *D. persimilis* and *D. pseudoobscura*. Here, we do not include the highly
286 polymorphic inversions of chromosome 3, where a complex series of overlapping inversions pre-
287 dates the estimated speciation timing of *D. persimilis* and *D. pseudoobscura*, resulting in large segments
288 of high, long-term LD (Aquadro, Weaver, Schaeffer, & Anderson, 1991; Fuller, Haynes, Richards, &
289 Schaeffer, 2017; Wallace, Detweiler, & Schaeffer, 2011). To consider the effects of inversions on
290 divergence, we contrast observed patterns within inversions to regions outside the inversions
291 (collinear) and to the subset of collinear regions that can be predicted to be reasonably freely-
292 recombining (denoted as $\text{collinear}_{\text{FR}}$). $\text{collinear}_{\text{FR}}$ excludes the 5 Mb windows adjacent to telomeric
293 and centromeric chromosome ends, which undergo very little crossing over (Andolfatto & Wall,
294 2003; Kulathinal, Bennett, Fitzpatrick, & Noor, 2008; Steviston & Noor, 2010). Similarly, $\text{collinear}_{\text{FR}}$
295 excludes regions within 2.5 Mb outside of inversion breakpoints, based on previous reports of
296 crossover suppression 1-2 Mb beyond inversion breakpoints (Kulathinal et al., 2009; Machado,
297 Haselkorn, & Noor, 2007; Steviston, Hoehn, & Noor, 2011).

298 First, confirming many previous studies (Kulathinal et al., 2009; Machado et al., 2007;
299 McGaugh & Noor, 2012; M. A. F. Noor, Garfield, Schaeffer, & Machado, 2007; Steviston et al.,
300 2011), we observed that *D. persimilis* vs *D. p. pseudoobscura* divergence is significantly higher in
301 inverted than collinear windows, regardless of whether the inverted regions are compared to all
302 collinear windows or to the $\text{collinear}_{\text{FR}}$ subset (Supplementary Table 3). Second, our inclusion of the
303 allopatric *D. persimilis* vs *D. p. bogotana* comparison reveals several interesting new patterns. Estimates
304 of divergence between *D. persimilis* and *D. p. bogotana* are consistently higher than estimates of
305 divergence between *D. persimilis* vs *D. p. pseudoobscura*, even in breakpoint-adjacent regions, as we
306 discuss further below. We also note that *D. persimilis* vs allopatric *D. p. bogotana* divergence is higher

307 in inverted than collinear windows on chromosomes 2 and XL (the difference is nonsignificant on
308 chromosome XR unless the comparison is restricted to collinear_{FR}; Supplementary Table 3).

309 Higher divergence in inverted vs collinear regions could be due to pre-speciation segregation
310 of inversion polymorphisms in the ancestral population or to interspecies gene flow homogenizing
311 collinear regions. Here, we focus on testing the latter, since previous work already provides evidence
312 for exchange between karyotypes due to inversion polymorphisms segregating in the ancestral
313 population. Briefly, the ages of the inversions examined here have been consistently inferred as pre-
314 dating the estimated divergence time of *D. pseudoobscura* and *D. persimilis* (Fuller et al. , 2018; Hey &
315 Nielsen, 2004; R. L. Wang & Hey, 1996). While we do not repeat these analyses in full, we note that
316 our estimates of average divergence within the inversions (Supplementary Table 3) are consistent
317 with previous accounts of the relative divergence and ages of the inversions (Fuller et al., 2018;
318 McGaugh & Noor, 2012; M. A. F. Noor et al., 2007). For both *D. persimilis* vs *D. p. pseudoobscura* and
319 *D. persimilis* vs *D. p. bogotana*, we compared measures of windowed divergence among the inverted
320 regions. Each pairwise comparison between the inversions yielded a significant difference wherein
321 XL > 2 > XR ($p < 0.0001$, Mann-Whitney U test; Supplementary Table 3). Given the evidence that
322 inversions were segregating in the ancestral population of these species, we test for evidence of post-
323 speciation gene flow and attempt to disentangle the timing of such gene flow.

324



325

326 **Figure 3 | Genome-wide divergence between species.** On the left, each of the 3 inversion-
 327 bearing chromosome arms are plotted from centromere (0) to telomere, inversion boundaries are
 328 shown with vertical black lines. D_{xy} per 50 kb window is plotted to show absolute divergence
 329 between *D. persimilis* and *D. p. bogotana* (red) and absolute divergence between *D. persimilis* vs *D. p.*
 330 *pseudoobscura* (blue). Boxplots (right) summarize these divergence estimates by region: Inverted,
 331 Collinear, and Collinear_{FR}. Collinear_{FR} is the subset of collinear positions predicted to be freely
 332 recombining (excludes the grayed-out positions near inversion breakpoints or chromosome ends).

333

334 **Evidence for early post-speciation exchange**

335 To test for evidence of gene flow after speciation but before the split of *D. p. pseudoobscura*
 336 and *D. p. bogotana* (Figure 1), we fit observed patterns of collinear region intergenic nucleotide
 337 variation in *D. persimilis* and *D. p. bogotana* to models of divergence in isolation, isolation-with-

338 migration (IM), and isolation-with-initial-migration (IIM) using maximum-likelihood estimation of
339 parameters under these models (Figure 2; Costa & Wilkinson-Herbots 2017). In traditional IM
340 models applied to infer gene flow, parameter estimates can be biased by the underlying assumption
341 that gene flow is constant. IIM specifically addresses this assumption by operating on the premise of
342 an initial period of gene flow followed by isolation. An IIM framework is appropriate for the *D.*
343 *persimilis* and *D. p. bogotana* comparison, given our knowledge that these taxa have been evolving in
344 allopatry for the past 150,000 years (S W Schaeffer & Miller, 1991). Indeed, a nested model
345 comparison to test the relative support among the models rejects the null hypothesis of divergence
346 in isolation and suggests that IIM models best fit the data (Table 1 and Supplementary Table 4). All
347 models allowing for migration and population size change gave a significantly better fit than a model
348 of strict divergence in isolation, and the log-likelihood of the data under the tested models was
349 maximized in the IIM2 scenario (Table 1 and Supplementary Table 4). The IIM2 model estimates
350 parameters under divergence with potentially asymmetric bidirectional gene flow until some
351 timepoint in the past and, unlike the IIM1 model, does not assume constant population sizes (Figure
352 2). We also considered models similar to IIM2, but assuming unidirectional gene flow between *D.*
353 *persimilis* and *D. p. bogotana* (IIM3 and IIM4). Nested model comparison supports the choice of any
354 of the three models with varying population sizes (IIM2, IIM3, or IIM4) over IIM1, and the
355 likelihood of IIM2 supports bidirectional gene flow (Table 1). An application of the Costa &
356 Wilkinson-Herbots (2017) framework to the sympatric *D. persimilis* and *D. p. pseudoobscura*
357 comparison can be found in Fuller et al. (2018), which also found the best fit to be an IIM model,
358 compatible with our results suggesting gene flow between the *D. persimilis* and *D. p. pseudoobscura*
359 lineages after speciation. Importantly, our application of this framework to the allopatric *D. persimilis*
360 and *D. p. bogotana* comparison demonstrates that a significant amount of this exchange likely
361 occurred prior to the split of *D. p. bogotana* (region 2 in Figure 1).

362 **Table 1** | Forward selection of the best model[†] of *D. persimilis* - *D. p. bogotana* divergence using the
 363 maximized log-likelihood (LogL) under each model in likelihood-ratio tests.

H ₀	H ₁	Deg. of Freedom	LogL H ₀	LogL H ₁	LRT Statistic	P-value
Iso	IM	2	-25511.23	-25492.84	36.78	1.031e-08
Iso	Iso2	2	-25511.23	-25467.66	87.14	1.196e-19
IM	IIM1	1	-25492.84	-25492.84	0	-
IM	IIM2	3	-25492.84	-25442.42	100.84	1.025e-21
Iso2	IIM2	3	-25467.66	-25442.42	50.48	6.313e-11
IIM1	IIM2	2	-25492.84	-25442.42	100.84	1.267e-22
IIM1	IIM3	1	-25492.84	-25447.73	90.22	2.131e-21
IIM1	IIM4	1	-25492.84	-25444.03	97.62	5.069e-23

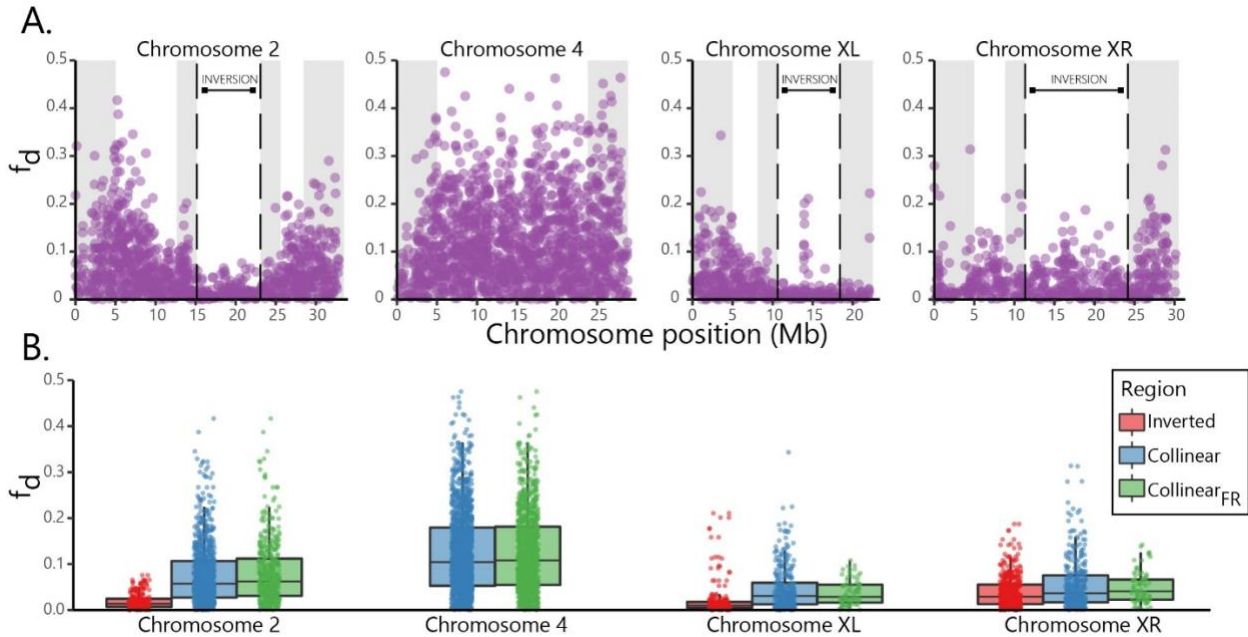
364 [†] See Figure 2 for illustration of the different models.

365 **Patterson's D-statistic and f_d suggest recent introgression**

366 Given the evidence for gene flow between *D. persimilis* and *D. pseudoobscura*, we next
 367 examined whether some of this gene flow was very recent (within the past 150,000 years). To
 368 contrast sympatric and allopatric subspecies of *D. pseudoobscura* in their similarity to *D. persimilis*, we
 369 applied Patterson's D-statistic and f_d (Martin et al., 2015) using the tree: (((*D. p. bogotana*, *D. p.*
 370 *pseudoobscura*), *D. persimilis*), *D. lowei*)). Patterson's D-statistic is an implementation of ABBA-BABA,
 371 which uses parsimony informative sites to test whether derived alleles ("B") in *D. persimilis* are shared
 372 with *D. p. bogotana* or with *D. p. pseudoobscura* at equal frequencies. Derived alleles in *D. persimilis* may
 373 be shared with *D. p. pseudoobscura* due to ancestral polymorphism, ancient gene flow (prior to the split
 374 of the two *D. pseudoobscura* subspecies), recent gene flow (since the split of the two *D. pseudoobscura*
 375 subspecies), or a combination of these factors. The null expectation is that the two phylogeny-
 376 discordant patterns, ABBA and BABA, should be present equally if ancestral polymorphism and
 377 ancient gene flow are the sole drivers of patterns of divergence. Gene flow between *D. p.*
 378 *pseudoobscura* and *D. persimilis* since the split of the two *D. pseudoobscura* subspecies (estimated at
 379 150,000 years ago: Schaeffer & Miller 1991) would promote an excess of ABBA over BABA
 380 patterns, particularly on freely recombining chromosomes. Indeed, ABBA sites exceed BABA sites

381 on all chromosomes (Supplementary Table 5), and chromosome 4 shows an unambiguously
382 significant excess of ABBA ($|Z\text{-score}| \geq 5$), suggesting that the phylogenetic relationship between
383 these four taxa does not fully explain the observed patterns of divergence and some very recent gene
384 exchange has occurred between the North American species. Furthermore, the genome wide z-score
385 for collinear regions is significant ($|Z\text{-score}| = 7.215$), and none of the z-scores for inverted regions
386 are significant (Supplementary Table 5).

387 Given the observed excess of ABBA over BABA sites throughout the genome, we next
388 applied f_d to quantify this excess in smaller genomic intervals. In comparison to D-statistics, f_d is less
389 affected by differences in effective population size and is better suited to identifying introgression
390 regions (Martin et al., 2015). The genome-wide patterns of f_d support the evidence of gene flow
391 between *D. p. pseudoobscura* and *D. persimilis*, particularly in the collinear regions of the genome
392 (**Error! Reference source not found.**). Inverted regions exhibit markedly lower f_d compared to
393 collinear regions (**Error! Reference source not found.**A). This difference is statistically significant
394 on all inversion-bearing chromosomes, regardless of whether the inverted regions are compared to
395 all collinear regions or just the conservative subset contained in $\text{collinear}_{\text{FR}}$ (**Error! Reference**
396 **source not found.**B; $p < 0.01$ for all comparisons, Mann-Whitney U).



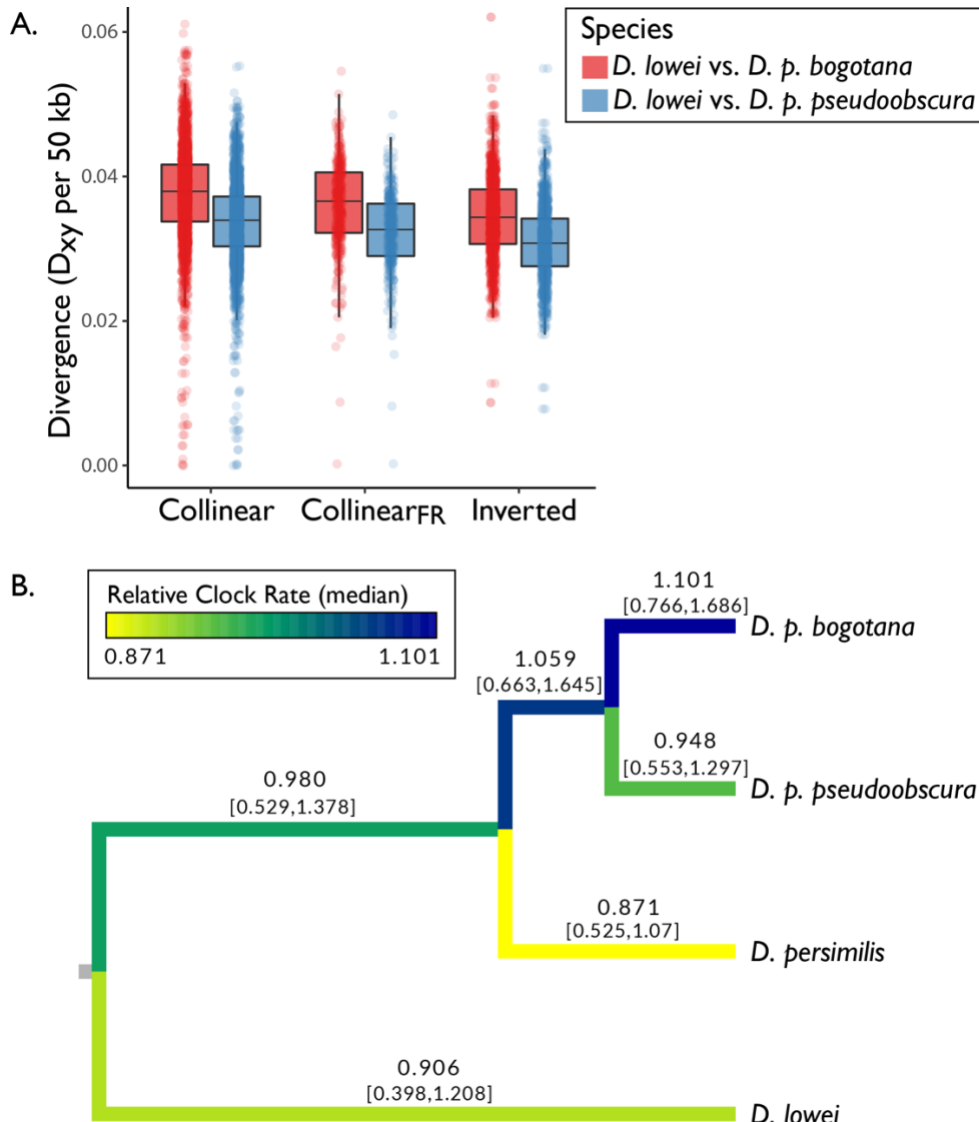
397
398 **Figure 4 | Signals of introgression along the genome.** (A) The estimated proportion of
399 introgression (f_d) between *D. pseudoobscura* and *D. persimilis* is shown in non-overlapping 100 SNP
400 windows along chromosomes 2, 4, XL, and XR. Inversion boundaries are shown with dashed black
401 lines, and collinear regions are grayed-out where they approach inversion breakpoints or
402 chromosome ends (windows excluded from Collinear_{FR}). (B) A summary of the introgression
403 estimates by region: Inverted, Collinear, and Collinear_{FR}.

404 **Gene flow may act alongside other evolutionary forces that contribute to patterns of**
405 **higher divergence in allopatry vs sympatry**

406 All three inversion-bearing chromosomes exhibit lower divergence in the *D. persimilis*:*D. p.*
407 *pseudoobscura* comparison vs the *D. persimilis*:*D. p. bogotana* comparison (Figure 3). Notably, this lower
408 divergence in the sympatric comparison is statistically significant for both the collinear and inverted
409 regions ($p < 0.001$ on each chromosome, Mann-Whitney U test). Divergence between the species
410 pairs in both inverted and collinear regions shows the magnitude of this difference (Figure 3). This
411 pattern is consistent across all strains: differentiation in the inverted regions between *D. persimilis*:*D.*
412 *p. bogotana* is higher than differentiation between *D. persimilis* and any of the North American *D. p.*
413 *pseudoobscura* genomes (Supplementary Figure 2).

414 The observation that divergence is lower in sympatry compared to allopatry even in the
415 inverted regions was not anticipated. A possible explanation for the lower divergence in the
416 sympatric species pair is that gene flow is homogenizing these species even in inverted regions.
417 Estimates of divergence between *D. persimilis* and *D. p. bogotana* are consistently higher than estimates
418 of divergence between *D. persimilis* vs *D. p. pseudoobscura*, even in breakpoint-adjacent regions (Figure
419 3). Though there is evidence that double crossovers and gene conversions occur within inversions,
420 and gene conversion may occur in regions adjacent to inversion breakpoints (Crown, Miller,
421 Sekelsky, & Hawley, 2018; Korunes & Noor, 2017, 2019; Stephen W Schaeffer & Anderson, 2005;
422 Steviston et al., 2011), an alternative explanation is that *D. p. bogotana* has experienced more
423 substitutions per site. Comparing each subspecies of *D. pseudoobscura* to the outgroup, *D. lowei*, we
424 note that divergence between *D. lowei* and *D. p. bogotana* is significantly greater than divergence
425 between *D. lowei* and *D. p. pseudoobscura* in both collinear and inverted regions (Figure 5A; $p < 1 \times 10^{-8}$
426 for each of the three examined regions, Mann-Whitney U tests). This difference in divergence is
427 unlikely to be explained by gene flow, since *D. lowei* does not produce hybrids with either subspecies
428 of *D. p. pseudoobscura*. Genome-wide comparison of the relative substitution rates (Tajima, 1993)
429 between the lineages reveals that *D. p. bogotana* has experienced significantly more substitutions per
430 site than *D. p. pseudoobscura* relative to the outgroup species, *D. lowei* (Supplementary Table 6). To
431 further explore the possibility of variable evolutionary rates among the lineages, we estimated
432 relative clock rates using a Bayesian multispecies coalescent method, StarBEAST2 (Ogilvie et al.,
433 2017). We find that the median estimated relative clock rate is highest in *D. p. bogotana* (Figure 5B).
434 While these results suggest that variable clock rates may explain some of the divergence patterns
435 among these lineages, we use caution in interpreting these results, as there is substantial uncertainty
436 inherent in clock estimation.

437



438

439 **Figure 5 | Divergence from the outgroup *D. lowei*.** (A) The distribution of windowed D_{xy} in
440 Inverted, Collinear, and Collinear_{FR} regions (summarized together from chromosomes 2, 4, XL, and
441 XR) showing divergence between *D. lowei* and each *D. pseudoobscura* subspecies: *D. p. bogotana* (red)
442 and *D. p. pseudoobscura* (blue). For each of the three examined regions, *D. lowei* and *D. p. bogotana* is
443 significantly greater than divergence between *D. lowei* and *D. p. pseudoobscura* ($p < 1 \times 10^{-8}$ for each
444 comparison, Mann-Whitney U test). (B) Relative clock rates per species obtained from the posterior
445 distribution from StarBEAST2. Median clock rates are displayed for each branch, with confidence
446 intervals in brackets representing the 95% highest posterior density.

447

448 ***Discussion***

449 Our model-based examination of gene flow and statistical tests for excess shared variation
450 found between *D. persimilis* and sympatric and allopatric subspecies of *D. pseudoobscura* indicates post-
451 speciation gene exchange, including both early post-speciation gene flow and gene flow within the
452 past ~150,000 years. Specifically, we interpret the excess of ABBA > BABA sites as evidence that *D.*
453 *p. pseudoobscura* and *D. persimilis* have exchanged genes in collinear regions since the split of *D. p.*
454 *bogotana*. The ABBA–BABA test is well-suited for considering the net effect of gene flow over large
455 genomic regions, since it leverages patterns from many loci and thus accounts for variance among
456 loci, while the related statistic, f_d , is better suited for application to genomic windows.

457 The observed patterns in f_d show reduced signals of introgression in inverted vs collinear
458 regions and raise interesting questions about why f_d varies along each inversion and between the
459 inversions. We expect that the amount of introgression within each inversion reflects the interplay of
460 the inversion's age, size, genic content, X vs autosomal differences, and other genomic features. For
461 example, the smaller length (~7 Mb) of the inversion on chromosome XL may result in less gene
462 flux due to the reduced possibility for double crossover compared to the longer inversion (~12 Mb)
463 on chromosome XR. Windows with high f_d values may also provide candidates for regions
464 experiencing adaptive introgression or other functionally important evolutionary processes. For
465 example, within the inversion of chromosome XL there are 4 windows with f_d greater than two
466 standard deviations from the chromosome wide mean of 0.04 (Supplementary Table 7). Though we
467 do not have a clear hypothesis about specific genetic variation that might be driving this pattern, we
468 note that our BLAST results suggest that there are numerous genes within the approximately 538 kb
469 region containing these windows, including several BLAST hits within the 4 high f_d windows
470 (Supplementary Table 7). These genes, or nearby genes, may be interesting candidates for future

471 work. Overall, patterns in f_d highlight several potential areas for future work and provide the key
472 finding of significantly lower f_d in inverted compared to collinear regions (**Error! Reference source**
473 **not found.**), supporting the idea that inversions have acted as barriers to gene flow.

474 This evidence that introgression is driving patterns of divergence between *D. pseudoobscura*
475 and *D. persimilis* is in agreement with previous reports of ongoing hybridization in these species
476 (Dobzhansky, 1973; Hey & Nielsen, 2004; Machado & Hey, 2003; J R Powell, 1983). Despite our
477 evidence for recent gene exchange, it appears that introgression is not the sole driver of patterns of
478 divergence between these species overall. While D-statistics and f_d suggest an excess of shared,
479 derived alleles across the genomes of *D. pseudoobscura* and *D. persimilis*, these statistics may be biased
480 by factors such as ancestral population structure and differences in effective population size (He,
481 Liang, & Zhang, 2020; Martin et al., 2015; Slatkin & Pollack, 2008). In comparison to Patterson's D-
482 statistic, f_d is less sensitive to local variation in recombination rate and divergence. However, it can
483 still be biased by regions of reduced interspecies divergence, which may distort tests for recent
484 introgression (Martin et al., 2015), so the conclusion of recent introgression would be tentative
485 based on these results alone. Here, we explore other important factors that might underlie the
486 observed patterns of divergence, with particular consideration of how these factors might confound
487 signals of recent introgression.

488 As seen in Figure 3 and in previous studies (Kulathinal et al., 2009), divergence is higher in
489 inverted vs collinear regions in this system. This difference holds for divergence between *D. persimilis*
490 and either *D. p. bogotana* or *D. p. pseudoobscura*. The lower observed divergence in sympatry compared
491 to allopatry even in the inverted regions is somewhat surprising given the expectation that
492 recombination in hybrids will be restricted in these inverted regions. This observation led us to
493 consider the possibility that the allopatric subspecies, *D. p. bogotana*, might have experienced more
494 nucleotide substitutions per site than the other taxa. Thus, we considered four non-mutually

495 exclusive factors that might contribute to the observed patterns of divergence with respect to
496 chromosomal arrangement: 1) the segregation of ancestral polymorphism (as advocated by Fuller *et*
497 *al.* (2018)), 2) increased ~~branch length~~ substitution rate (branch length) in the allopatric *D. p. bogotana*,
498 3) gene flow prior to the split of *D. p. bogotana*, and 4) recent/ongoing gene flow (the latter two
499 discussed in Powell 1983; Wang & Hey 1996; Wang *et al.* 1997; Noor *et al.* 2001, 2007; Machado &
500 Hey 2003; Hey & Nielsen 2004; Machado *et al.* 2007; Kulathinal *et al.* 2009; McGaugh & Noor 2012).
501 Achieving a cohesive view of the role of inversions in species divergence relies on considering the
502 combined effects of these factors.

503 While it is challenging to disentangle these factors, we suggest that an important area for
504 future work will be developing statistical approaches to summarize patterns of divergence while
505 adjusting for other evolutionary dynamics. For example, D_{xy} could potentially be leveraged to
506 provide insight into the effects of introgression on divergence after adjusting for differences in
507 branch lengths. For the sympatric pair *D. persimilis* vs *D. p. pseudoobscura*, any difference in D_{xy} in
508 inverted regions compared to collinear regions could be due to the segregation of ancestral inversion
509 polymorphism or to post-speciation genetic exchange. In contrast, any difference in D_{xy} in inverted
510 regions compared to collinear regions in the allopatric pair *D. persimilis* vs *D. p. bogotana* could be
511 driven by the segregation of ancestral inversion polymorphism or by post-speciation gene flow prior
512 to the split of *D. p. bogotana*. This comparison will not reflect any recent gene flow, since *D. p.*
513 *bogotana* has evolved in allopatry for the past 150,000 years.

514 To explore how this contrast might be used to isolate the effects of recent introgression on
515 divergence, we compared the divergence of each *D. pseudoobscura* subspecies from *D. persimilis* to the
516 divergence of each *D. pseudoobscura* subspecies from *D. lowei* using the following equation to define
517 the “introgression effect”: $(D_{xy} [D. persimilis:D.p.bogotana] - D_{xy} [D. persimilis:D.p.pseudo.]) - (D_{xy}$
518 $[D. lowei:D.p.bogotana] - D_{xy} [D. lowei:D.p.pseudo.])$. The first half of this equation should include the

519 effects of branch length in *D. p. bogotana* and the effects of any introgression between *D. pseudoobscura*
520 and *D. persimilis* (Supplementary Figure 3A). Since *D. lowei* does not hybridize with any of these
521 species, the second half of the equation should reflect only the effects of branch length in *D. p.*
522 *bogotana*. Thus, we propose that the difference between these terms should subtract effects of
523 evolutionary rate, leaving effects of recent introgression.

524 Such a proposed "introgression effect" statistic may be one potential strategy for examining
525 the relative influence of recent introgression on the reduction in *D. persimilis* vs *D. pseudoobscura*
526 divergence in sympatry vs allopatry. Applying this strategy to the present data, we note that inverted
527 vs. collinear regions differ significantly, suggesting that introgression has influenced divergence in
528 the collinear regions more so than the inverted regions (Supplementary Figure 3B; $p < 1 \times 10^{-8}$, all
529 inverted vs collinear comparisons, Mann-Whitney U test) and providing evidence that branch-length
530 differences alone are insufficient to fully explain the patterns of divergence. As we are interested in
531 whether, when, and how chromosomal inversions are contributing to patterns of divergence by
532 suppressing gene flow, the observed difference suggests that this strategy may provide a useful way
533 to consider the relative contribution of recent introgression compared to ancestral polymorphism
534 and branch length in species groups where similar allopatric-sympatric contrasts could be conducted.
535 However, we emphasize that the behavior of this kind of statistic remains to be explored. While any
536 conclusions based on this strategy are tentative at best, we hope that Supplementary Figure 3
537 stimulates discussion on future approaches.

538 Taken together, our results suggest that contributions from recent gene flow only partially
539 explain observed divergence patterns. Patterns of divergence between *D. persimilis* and *D.*
540 *pseudoobscura* may be explained by a combination of segregating ancestral polymorphism and post-
541 speciation gene flow. We applied a model-based approach to investigate the timing of gene flow
542 between *D. persimilis* and *D. pseudoobscura*. Our results suggest that an isolation-with-initial-migration

543 model best explains the divergence of *D. persimilis* and *D. p. bogotana* when compared to a model of
544 strict isolation. This result provides further evidence for gene flow between *D. persimilis* and *D.*
545 *pseudoobscura*, and it suggests that some of this gene flow occurred prior to the split of *D. p. bogotana*
546 and remains detectable in observed genetic patterns.

547 Our results question interpretations from earlier studies of this system. Given that *D. p.*
548 *bogotana* can be reasonably assumed to not be currently exchanging genes with either *D. persimilis* or
549 *D. p. pseudoobscura* (S W Schaeffer & Miller, 1991; R. L. Wang et al., 1997), *D. persimilis*: *D. p. bogotana*
550 divergence was argued to be a suitable “negative control” for examining the effect of recent
551 hybridization between *D. persimilis* and *D. p. pseudoobscura* (Brown et al., 2004). By this argument, the
552 effect of recent gene flow can be estimated by an allopatric vs sympatric comparison of the
553 difference in divergence (whether in DNA sequence or in phenotype) in inverted regions to
554 divergence in collinear regions. Specifically, Brown *et al.* (2004) and Chang and Noor (2007) inferred
555 multiple hybrid sterility factors between *D. p. bogotana* and *D. persimilis* that did not distinguish North
556 American *D. p. pseudoobscura* and *D. persimilis* (Brown et al., 2004; Chang & Noor, 2007). Similarly,
557 Kulathinal *et al.* (2009) observed significantly greater sequence difference between *D. p. bogotana* and
558 *D. persimilis* than between *D. p. pseudoobscura* and *D. persimilis*. In both cases, the authors interpreted
559 the difference to result from recent homogenization of the collinear regions in the latter pair. Based
560 on our findings, we suggest this difference may result at least in part from the accelerated rate of
561 divergence in *D. p. bogotana* (Figure 5, Supplementary Table 6).

562 Notably, there are also significant differences in demographic history and environmental
563 factors among the lineages. *D. p. bogotana* may have experienced a population bottleneck upon
564 colonization of South America leading to a subsequently small effective population size (Machado et
565 al., 2002; S W Schaeffer & Miller, 1991; R. L. Wang & Hey, 1996). These past reports of smaller
566 effective population size in *D. p. bogotana* are corroborated by our maximum-likelihood estimates

567 under all considered models of divergence (Supplementary Table 4, where θ_B reflects the relative
568 population size of *D. p. bogotana* during the stage with genetic exchange between subpopulations, and
569 θ_{C2} reflects the relative population size of *D. p. bogotana* during the isolation stage.) Additionally, the
570 process of genetic divergence that shapes alleles responsible for local adaptation and hybrid
571 incompatibility can extend deep into the history of the species. In fact, the influence of inversions
572 on the divergence of a species pair can predate the split of the species. Inversion polymorphisms in
573 the ancestral population of a species pair can contribute to patterns of higher sequence
574 differentiation between species in those inverted regions (Fuller et al., 2018). Separating these effects
575 requires an understanding of the timing and extent of introgression, which can only be understood
576 with an appreciation for the evolutionary processes occurring in each of the taxa at hand. Overall,
577 we caution that simple allopatry-sympatry comparisons can easily be misleading, and the population
578 histories and rates of evolution of the examined species should be carefully considered. We present
579 evidence of gene flow between *D. pseudoobscura* and *D. persimilis* both before and after the split of *D.*
580 *p. bogotana* from North American *D. p. pseudoobscura*. Though there are many remaining questions
581 about how inversions shape divergence, our findings build on the large body of work in this classic
582 system to provide evidence that inversions have contributed to the divergence of *D. pseudoobscura*
583 and *D. persimilis* over multiple distinct periods during their speciation: 1) early in the speciation
584 continuum of *D. pseudoobscura* and *D. persimilis*, due to segregation of inversions in the ancestral
585 population, 2) post-speciation gene flow prior to the split of *D. p. bogotana*, and 3) recent gene flow.

586

587

588 **AUTHOR CONTRIBUTIONS**

589 KLK and MAFN were responsible for the project's conception and design, in consultation with
590 CAM. KLK performed the analyses and prepared the manuscript with essential feedback and
591 revisions from MAFN and CAM.

592

593 **ACKNOWLEDGMENTS**

594 The authors thank all members of the Noor lab for helpful discussions and also thank Z. Fuller, R.
595 Corbett-Detig, B. Emerson, and three anonymous reviewers for their thoughtful feedback on the
596 manuscript. KLK was supported by the National Science Foundation Graduate Research
597 Fellowship Program under grant no. DGE-1644868, and this work was additionally supported by
598 National Science Foundation grants DEB- 1754022 and DEB-1754439 to MAFN, and MCB-
599 1716532 and DEB-1754572 to CAM.

References

Altschul, S. F., Gish, W., Miller, W., Myers, E. W., & Lipman, D. J. (1990). Basic local alignment search tool. *Journal of Molecular Biology*, 215(3), 403–410. Retrieved from <http://www.sciencedirect.com/science/article/pii/S0022283605803602>

Andolfatto, P., & Wall, J. D. (2003). Linkage disequilibrium patterns across a recombination gradient in African *Drosophila melanogaster*. *Genetics*, 165(3), 1289–1305. Retrieved from <http://www.genetics.org/content/165/3/1289.short>

Aquadro, C. F., Weaver, A. L., Schaeffer, S. W., & Anderson, W. W. (1991). Molecular evolution of inversions in *Drosophila pseudoobscura*: The amylase gene region. *Proceedings of the National Academy of Sciences of the United States of America*, 88(1), 305–309. doi: 10.1073/pnas.88.1.305

Ayala, F. J., & Coluzzi, M. (2005). Chromosome speciation: humans, *Drosophila*, and mosquitoes. *Proceedings of the National Academy of Sciences*, 102 Suppl(suppl 1), 6535–6542. doi: 10.1073/pnas.0501847102

Beckenbach, A. T., Wei, Y. W., & Liu, H. (1993). Relationships in the *Drosophila obscura* species group, inferred from mitochondrial cytochrome oxidase II sequences. *Molecular Biology and Evolution*, 10(3), 619–634. doi: 10.1093/oxfordjournals.molbev.a040034

Brown, K. M., Burk, L. M., Henagan, L. M., & Noor, M. A. F. (2004). A test of the chromosomal rearrangement model of speciation in *Drosophila pseudoobscura*. *Evolution*, 58(8), 1856–1860. Retrieved from <http://www.ncbi.nlm.nih.gov/pubmed/15446438>

Butlin, R. K. (2005). Recombination and speciation. *Molecular Ecology*, 14(9), 2621–2635. doi: 10.1111/j.1365-294X.2005.02617.x

Chang, A. S., & Noor, M. A. F. (2007). The genetics of hybrid male sterility between the allopatric species pair *Drosophila persimilis* and *D. pseudoobscura bogotana*: dominant sterility alleles in collinear autosomal regions. *Genetics*, 176(1), 343–349. doi: 10.1534/genetics.106.067314

Costa, R. J., & Wilkinson-Herbots, H. (2017). Inference of gene flow in the process of speciation: An efficient maximum-likelihood method for the isolation-with-initial-migration model. *Genetics*, 205(4), 1597–1618. doi: 10.1534/genetics.116.188060

Crown, K. N., Miller, D. E., Sekelsky, J., & Hawley, R. S. (2018). Local inversion heterozygosity alters recombination throughout the genome. *Current Biology*, 28(18), 2984–2990. doi: 10.1016/j.cub.2018.07.004

Dobzhansky, T. (1973). Is there gene exchange between *Drosophila pseudoobscura* and *Drosophila persimilis* in their natural habitats? Retrieved October 19, 2015, from The American Naturalist website: http://www.jstor.org/stable/2459801?seq=1#page_scan_tab_contents

Dobzhansky, T., & Epling, C. (1944). Contributions to the genetics, taxonomy, and ecology of *Drosophila pseudoobscura* and its relatives. *Carnegie Institute of Washington*, 544, 1–46.

Feder, J. L., Gejji, R., Powell, T. H. Q., & Nosil, P. (2011). Adaptive chromosomal divergence driven by mixed geographic mode of evolution. *Evolution*, 65(8), 2157–2170. doi: 10.1111/j.1558-5646.2011.01321.x

Fuller, Z. L., Haynes, G. D., Richards, S., & Schaeffer, S. W. (2017). Genomics of natural

populations: evolutionary forces that establish and maintain gene arrangements in *Drosophila pseudoobscura*. *Molecular Ecology*, 26(23), 6539–6562. doi: 10.1111/mec.14381

Fuller, Z. L., Leonard, C. J., Young, R. E., Schaeffer, S. W., & Phadnis, N. (2018). Ancestral polymorphisms explain the role of chromosomal inversions in speciation. *PLoS Genetics*, 14(7), e1007526. doi: 10.1371/journal.pgen.1007526

Guerrero, R. F., Rousset, F., & Kirkpatrick, M. (2012). Coalescent patterns for chromosomal inversions in divergent populations. *Philosophical Transactions of the Royal Society B*, 367(1587), 430–438. doi: 10.1098/rstb.2011.0246

He, C., Liang, D., & Zhang, P. (2020). Asymmetric Distribution of Gene Trees Can Arise under Purifying Selection If Differences in Population Size Exist. *Molecular Biology and Evolution*, 37(3), 881–892. doi: 10.1093/molbev/msz232

Heed, W. B., Crumpacker, D. W., & Ehrman, L. (1969). *Drosophila lowei*, a new American member of the *Obscura* species group1,2. *Annals of the Entomological Society of America*, 62(2), 388–393. doi: 10.1093/aesa/62.2.388

Hey, J., & Nielsen, R. (2004). Multilocus methods for estimating population sizes, migration rates and divergence time, with applications to the divergence of *Drosophila pseudoobscura* and *D. persimilis*. *Genetics*, 167(2), 747–760. doi: 10.1534/genetics.103.024182

Jackson, B. C. (2011). Recombination-suppression: how many mechanisms for chromosomal speciation? *Genetica*, 139(3), 393–402. doi: 10.1007/s10709-011-9558-0

Korunes, K. L., Myers, R. B., Hardy, R., & Noor, M. A. F. (2020). PseudoBase: A genomic visualization and exploration resource for the *Drosophila pseudoobscura* subgroup. *Fly*. doi: 10.1080/19336934.2020.1864201

Korunes, K. L., & Noor, M. A. F. (2017). Gene conversion and linkage: Effects on genome evolution and speciation. *Molecular Ecology*, 26(1), 351–364. doi: 10.1111/mec.13736

Korunes, K. L., & Noor, M. A. F. (2019). Pervasive gene conversion in chromosomal inversion heterozygotes. *Molecular Ecology*, 28(6), 1302–1315. doi: 10.1111/mec.14921

Kulathinal, R. J., Bennett, S. M., Fitzpatrick, C. L., & Noor, M. A. F. (2008). Fine-scale mapping of recombination rate in *Drosophila* refines its correlation to diversity and divergence. *Proceedings of the National Academy of Sciences*, 105(29), 10051–10056. doi: 10.1073/pnas.0801848105

Kulathinal, R. J., Stevenson, L. S., & Noor, M. A. F. (2009). The genomics of speciation in *Drosophila*: diversity, divergence, and introgression estimated using low-coverage genome sequencing. *PLoS Genetics*, 5(7), e1000550. doi: 10.1371/journal.pgen.1000550

Langley, C. H., Lazzaro, B. P., Phillips, W., Heikkinen, E., & Braverman, J. M. (2000). Linkage disequilibria and the site frequency spectra in the su(s) and su(wa) regions of the *Drosophila melanogaster* X chromosome. *Genetics*, 156(4), 1837–1852. Retrieved from <http://www.genetics.org/content/156/4/1837.short>

Li, H., & Durbin, R. (2009). Fast and accurate short read alignment with Burrows-Wheeler Transform. *Bioinformatics*, 25(14), 1754–1760. doi: 10.1093/bioinformatics/btp324

Li, H., Handsaker, B., Wysoker, A., Fennell, T., Ruan, J., Homer, N., ... Durbin, R. (2009). The Sequence Alignment/Map format and SAMtools. *Bioinformatics*, 25(16), 2078–2079. doi:

10.1093/bioinformatics/btp352

Lowry, D. B., & Willis, J. H. (2010). A widespread chromosomal inversion polymorphism contributes to a major life-history transition, local adaptation, and reproductive isolation. *PLoS Biology*, 8(9), e1000500. doi: 10.1371/journal.pbio.1000500

Machado, C. A., Haselkorn, T. S., & Noor, M. A. F. (2007). Evaluation of the genomic extent of effects of fixed inversion differences on intraspecific variation and interspecific gene flow in *Drosophila pseudoobscura* and *D. persimilis*. *Genetics*, 175(3), 1289–1306. doi: 10.1534/genetics.106.064758

Machado, C. A., & Hey, J. (2003). The causes of phylogenetic conflict in a classic *Drosophila* species group. *Proceedings of the Royal Society B: Biological Sciences*, 270(1520), 1193–1202. doi: 10.1098/rspb.2003.2333

Machado, C. A., Kliman, R. M., Markert, J. A., & Hey, J. (2002). Inferring the history of speciation from multilocus DNA sequence data: The case of *Drosophila pseudoobscura* and close relatives. *Molecular Biology and Evolution*, 19(4), 472–488. doi: 10.1093/oxfordjournals.molbev.a004103

Malinsky, M., Matschiner, M., & Svardal, H. (2020). Dsuite - fast D-statistics and related admixture evidence from VCF files. *BioRxiv*. doi: 10.1101/634477

Mallet, J. (2005). Hybridization as an invasion of the genome. *Trends in Ecology & Evolution*, 20(5), 229–237. doi: 10.1016/j.tree.2005.02.010

Manoukis, N. C., Powell, J. R., Touré, M. B., Sacko, A., Edillo, F. E., Coulibaly, M. B., ... Besansky, N. J. (2008). A test of the chromosomal theory of ecotypic speciation in *Anopheles gambiae*. *Proceedings of the National Academy of Sciences of the United States of America*, 105(8), 2940–2945. doi: 10.1073/pnas.0709806105

Martin, S. H., Davey, J. W., & Jiggins, C. D. (2015). Evaluating the use of ABBA–BABA statistics to locate introgressed loci. *Molecular Biology and Evolution*, 32(1), 244–257. doi: 10.1093/molbev/msu269

McGaugh, S. E., Heil, C. S. S., Manzano-Winkler, B., Loewe, L., Goldstein, S., Himmel, T. L., & Noor, M. A. F. (2012). Recombination modulates how selection affects linked sites in *Drosophila*. *PLoS Biology*, 10(11), e1001422. doi: 10.1371/journal.pbio.1001422

McGaugh, S. E., & Noor, M. A. F. (2012). Genomic impacts of chromosomal inversions in parapatric *Drosophila* species. *Philosophical Transactions of the Royal Society B: Biological Sciences*, 367(1587), 422–429. doi: 10.1098/rstb.2011.0250

McKenna, A., Hanna, M., Banks, E., Sivachenko, A., Cibulskis, K., Kernytsky, A., ... DePristo, M. A. (2010). The Genome Analysis Toolkit: a MapReduce framework for analyzing next-generation DNA sequencing data. *Genome Research*, 20(9), 1297–1303. doi: 10.1101/gr.107524.110

Michel, A. P., Sim, S., Powell, T. H. Q., Taylor, M. S., Nosil, P., & Feder, J. L. (2010). Widespread genomic divergence during sympatric speciation. *Proceedings of the National Academy of Sciences of the United States of America*, 107(21), 9724–9729. doi: 10.1073/pnas.1000939107

Noor, M. A. F., Garfield, D. A., Schaeffer, S. W., & Machado, C. A. (2007). Divergence between the *Drosophila pseudoobscura* and *D. persimilis* genome sequences in relation to chromosomal

inversions. *Genetics*, 177(3), 1417–1428. doi: 10.1534/genetics.107.070672

Noor, M. A., Grams, K. L., Bertucci, L. A., & Reiland, J. (2001). Chromosomal inversions and the reproductive isolation of species. *Proceedings of the National Academy of Sciences*, 98(21), 12084–12088. doi: 10.1073/pnas.221274498

Ogilvie, H. A., Bouckaert, R. R., & Drummond, A. J. (2017). StarBEAST2 Brings Faster Species Tree Inference and Accurate Estimates of Substitution Rates. *Molecular Biology and Evolution*, 34(8), 2101–2114. doi: 10.1093/molbev/msx126

Patterson, N., Moorjani, P., Luo, Y., Mallick, S., Rohland, N., Zhan, Y., ... Reich, D. (2012). Ancient admixture in human history. *Genetics*, 192(3), 1065–1093. doi: 10.1534/genetics.112.145037

Payseur, B. A., & Rieseberg, L. H. (2016). A genomic perspective on hybridization and speciation. *Molecular Ecology*, 25(11), 2337–2360. doi: 10.1111/mec.13557

Powell, J R. (1983). Interspecific cytoplasmic gene flow in the absence of nuclear gene flow: Evidence from *Drosophila*. *Proceedings of the National Academy of Sciences*, 80(2), 492–495. Retrieved from <http://www.ncbi.nlm.nih.gov/pmc/articles/PMC373404/>

Powell, Jeffrey R. (1992). Inversion polymorphisms in *Drosophila pseudoobscura* and *Drosophila persimilis*. *Drosophila Inversion Polymorphism*, 73–126.

Purcell, S., Neale, B., Todd-Brown, K., Thomas, L., Ferreira, M. A. R., Bender, D., ... Sham, P. C. (2007). PLINK: a tool set for whole-genome association and population-based linkage analyses. *American Journal of Human Genetics*, 81(3), 559–575. doi: 10.1086/519795

Rambaut, A. (2018). *FigTree v1.4.4*.

Samuk, K., Manzano-Winkler, B., Ritz, K. R., & Noor, M. A. F. (2020). Natural selection shapes variation in genome-wide recombination rate in *Drosophila pseudoobscura*. *Current Biology*, 30(8), 1517–1528.E6. doi: 10.1016/j.cub.2020.03.053

Schaeffer, S W, & Miller, E. L. (1991). Nucleotide sequence analysis of *Adh* genes estimates the time of geographic isolation of the Bogota population of *Drosophila pseudoobscura*. *Proceedings of the National Academy of Sciences*, 88(14), 6097–6101. doi: 10.1073/PNAS.88.14.6097

Schaeffer, Stephen W., Bhutkar, A., McAllister, B. F., Matsuda, M., Matzkin, L. M., O’Grady, P. M., ... Kaufman, T. C. (2008). Polytene chromosomal maps of 11 *Drosophila* species: The order of genomic scaffolds inferred from genetic and physical maps. *Genetics*, 179(3), 1601–1655. doi: 10.1534/genetics.107.086074

Schaeffer, Stephen W, & Anderson, W. W. (2005). Mechanisms of genetic exchange within the chromosomal inversions of *Drosophila pseudoobscura*. *Genetics*, 171(4), 1729–1739. doi: 10.1534/genetics.105.041947

Slatkin, M., & Pollack, J. L. (2008). Subdivision in an ancestral species creates asymmetry in gene trees. *Molecular Biology and Evolution*, 25(10), 2241–2246. doi: 10.1093/molbev/msn172

Stevison, L. S., Hoehn, K. B., & Noor, M. A. F. (2011). Effects of inversions on within- and between-species recombination and divergence. *Genome Biology and Evolution*, 3, 830–841. doi: 10.1093/gbe/evr081

Stevison, L. S., & Noor, M. A. F. (2010). Genetic and evolutionary correlates of fine-scale recombination rate variation in *Drosophila persimilis*. *Journal of Molecular Evolution*, 71(5–6), 332–345. doi: 10.1007/s00239-010-9388-1

Tajima, F. (1993). Simple methods for testing the molecular evolutionary clock hypothesis. *Genetics*, 135(2).

Taylor, S. A., & Larson, E. L. (2019, February 1). Insights from genomes into the evolutionary importance and prevalence of hybridization in nature. *Nature Ecology and Evolution*, Vol. 3, pp. 170–177. Nature Publishing Group. doi: 10.1038/s41559-018-0777-y

Van der Auwera, G. A., Carneiro, M. O., Hartl, C., Poplin, R., del Angel, G., Levy-Moonshine, A., ... DePristo, M. A. (2013). From FastQ data to high-confidence variant calls: The Genome Analysis Toolkit best practices pipeline. *Current Protocols in Bioinformatics*, 43(1), 11.10.1-11.10.33. doi: 10.1002/0471250953.bi1110s43

Wallace, A. G., Detweiler, D., & Schaeffer, S. W. (2011). Evolutionary History of the Third Chromosome Gene Arrangements of *Drosophila pseudoobscura* Inferred from Inversion Breakpoints. *Molecular Biology and Evolution*, 28(8), 2219–2229. doi: 10.1093/molbev/msr039

Wang, R. L., & Hey, J. (1996). The speciation history of *Drosophila pseudoobscura* and close relatives: inferences from DNA sequence variation at the period locus. *Genetics*, 144(3), 1113–1126. Retrieved from <http://www.genetics.org/content/144/3/1113.abstract>

Wang, R. L., Wakeley, J., & Hey, J. (1997). Gene flow and natural selection in the origin of *Drosophila pseudoobscura* and close relatives. *Genetics*, 147(3), 1091–1106. Retrieved from <http://www.genetics.org/content/147/3/1091.short>

Wang, Y., & Hey, J. (2010). Estimating divergence parameters with small samples from a large number of loci. *Genetics*, 184(2), 363–379. doi: 10.1534/genetics.109.110528

Yang, Z. (2002). Likelihood and Bayes estimation of ancestral population sizes in hominoids using data from multiple loci. *Genetics*, 162(4), 1811–1823. Retrieved from <http://www.ncbi.nlm.nih.gov/pubmed/12524351>